



Comparison between Three Algorithms in Predicting the Location of Accessory Pathway by 12 Lead Surface ECG in Wolff-Parkinson-White Syndrome Patients

Waleed Abd Allah Roshdy ^{a*}, Seham Fahmy Badr ^a,
Hanan Kamel Kassem ^a, Raghda Ghonimy Elsheikh ^a
and Mervat Abol Maaty Nabih ^a

^a Cardiovascular Medicine Department, Faculty of Medicine, Tanta University, Tanta, Egypt.

Authors' contributions

This work was carried out in collaboration among all authors. All authors read and approved the final manuscript.

Article Information

DOI: 10.9734/JAMMR/2022/v34i244917

Open Peer Review History:

This journal follows the Advanced Open Peer Review policy. Identity of the Reviewers, Editor(s) and additional Reviewers, peer review comments, different versions of the manuscript, comments of the editors, etc are available here: <https://www.sdiarticle5.com/review-history/94909>

Original Research Article

Received: 18/10/2022

Accepted: 22/12/2022

Published: 27/12/2022

ABSTRACT

Background: Wolff-Parkinson-White (WPW) syndrome, a pre-excitation condition that develops in 0.1-0.3% of the overall population, is brought on by the existence of an accessory atrioventricular circuit. With varied levels of difficulty and accuracy, many algorithms have been put forward for localizing accessory pathway (AP) utilizing 12-lead ECG analysis. This study aimed to compare between three algorithms in predicting where the accessory circuit is located in individuals with Wolff-Parkinson-White syndrome using a 12-lead surface ECG guided by successful ablation site.

*Corresponding author: E-mail: dr.n.badawy@gmail.com;

Methods: The research included 100 people with Wolff-Parkinson-White syndrome and was prospective cross-sectional in design. The patients were presented to the arrhythmia clinics at the Cardiology Departments in Tanta University Hospitals and Ain Shams University Hospitals (El-Demerdash hospital) and who were planned for electrophysiological study and radiofrequency ablation between July 2019 and July 2021. The ECG was analyzed and compared using the three selected algorithms and fluoroscopy was used to identify the location of a successful ablation at the time of catheter ablation. A complete electrophysiological study was done for exact localization of the accessory pathway.

Results: No major difference between the three algorithms in total accuracy was found, but as regard different AP locations, there was difference in sensitivity and specificity for each location between the three algorithms.

Conclusions: Arruda & d'Avila's approach was the most effective at predicting left-sided accessory pathways, while d'Avila then our proposed algorithm were the best algorithms for prediction of accessory pathways at right-sided. The best algorithms for detection of anteroseptal and mid-septal accessory pathways were our proposed algorithm and Arruda.

Keywords: Algorithm; accessory pathway; surface ECG; Wolff-Parkinson-White syndrome.

1. INTRODUCTION

Wolff-Parkinson-White (WPW) syndrome, a pre-excitation condition that develops in 0.1-0.3% of the overall population, is brought on by the existence of an accessory atrioventricular circuit. Tachyarrhythmia develops in 30–60% of these people during the course of their lifespan [1].

The WPW syndrome is a type of ventricular preexcitation in which a portion of the ventricular myocardium is depolarized earlier than usual through one or even more accessory pathways (APs) which circumvent the atrioventricular (AV) node, creating a direct connection between the atrium and the ventricle. This condition is characterised by an ECG with a delta wave, a short PR interval, a wide QRS complex, and occurrences of paroxysmal tachycardia [2]. Radiofrequency catheter ablation is advised as a class I therapeutic intervention in current treatment recommendations and has been shown to be a successful and curative intervention for WPW syndrome coupled with tachyarrhythmia. Therefore, it is crucial for clinical purposes to forecast an AP exact location before the ablation process [3]. To reduce the length of the procedure and the fluoroscopy, non-invasive diagnostic methods are employed to identify the AP with high precision prior to catheter ablation. In this context, body surface potential mapping, radioactive ventriculography, and 12-lead ECG have all been investigated. (1) A number of algorithms with differing levels of difficulty and accuracy have already been developed for identifying AP utilizing 12-lead ECG analysis [4]. The majority of them are based on an assessment of the shape

of delta waves. But because of their complexity, it may often be difficult to determine the delta wave form precisely. The accuracy of certain algorithm, which is based on the QRS polarity, on the other hand, has been documented, although it is still restricted [5].

2. METERIALS AND METHODS

The study was prospective cross-sectional study conducted on 100 Wolff-Parkinson-White syndrome patients presented to the arrhythmia clinics at the cardiology departments in Tanta University Hospitals and Ain Shams University Hospitals (El-Demerdash hospital) and who were planned for electrophysiological study and radiofrequency ablation between July 2019 and July 2021.

- Written informed permission was acquired from each research participant after explanation of the benefits and possible risks of the procedure and how we overcame these risks.
- Each patient's file had a code number that contained all investigations, thus all of the patients' data was strictly confidential, and privacy was granted.

2.1 Inclusion Criteria

All patients who fulfill the following:

1. Manifest preexcitation on 12 leads surface ECG.
2. Candidates planned for electrophysiological study and ablation.

3. Successful electrophysiological study and ablation.

2.2 Exclusion Criteria

1. Failed radiofrequency ablation.
2. Multiple accessory pathways.
3. Patients with complex congenital heart defects.

2.3 Type of Interventions

All cases included in this study were subjected to the following

❖ Full history taking including:

1. Age and gender.
2. Assessment of cardiovascular risk factors
 - Hypertension: which is defined as office systolic blood pressure values ≥ 140 mmHg and/or diastolic blood pressure (DBP) values ≥ 90 mmHg. [6]
 - Diabetes: according to American Diabetic Association 2019, diabetes is defined as fasting plasma glucose ≥ 126 mg/dL (7.0 mmol/L) or 2-hour plasma glucose ≥ 200 mg/dL (11.1 mmol/L) or HbA1c ≥ 6.5 % (48 mmol/mol) or random plasma glucose ≥ 11.1 mmol/L (≥ 200 mg/dL) plus symptoms [7].
 - Smoking
3. History of concomitant diseases (thyroid, renal and hepatic disorders).
4. Any medications the patient is taking for cardiac or non-cardiac purposes
5. Symptoms related to arrhythmia were assessed, e.g.
 - Palpitation
 - Dizziness
 - Presyncope
 - Syncope, which was described as an abrupt, temporary loss of consciousness and postural tension brought on by global cerebral

hypoperfusion and followed by a spontaneous full recovery with no neurologic consequences [8].

- Chest pain

❖ Complete clinical examination

- Pulse rate and regularity, and blood pressure.
- General examination.
- Local cardiac examination.

❖ Laboratory investigations:

(Complete blood picture {CBC}, liver function tests {SGPT, SGOT}, random glucose level, renal function tests {urea/creatinine}, thyroid stimulation hormone {TSH}, prothrombin time {PT} and international normalized ratio {INR}.

❖ Electrocardiogram (ECG):

12 Lead ECG recorded at paper speed of 25 mm/s and a gain of 10 mm/mV was performed before the electrophysiological study. The ECG was analyzed and compared using the three selected algorithms:

2.3.1 Arruda algorithm [9]

Based on the examination of the delta wave polarization in leads I, II, avF, and V1 and the analysis of the R/S ratio in leads III and V1, Arruda et al. [9] created an algorithm. They identified 13 distinct places around the mitral and tricuspid valves.

2.3.2 d' Avila algorithm [10]

d'Avila et al. [10] developed an algorithm which depends on QRS polarity in leads V1, III, aVL, II, and V2 to localize the accessory pathways. Their algorithm described 8 locations.

2.3.3 Proposed algorithm

This algorithm depends on the R wave progression in the chest leads and on the delta wave polarity in leads I, aVL, II, III, avF, and then on the R/S ratio in lead V₁.

This algorithm consists of 2 parts, crude and fine.

The crude algorithm consists of:

- Analysis of the delta wave III/avF
 - If positive → anterior location (LA, AS or RA)
 - If negative → posterior location (LP, PS or RP)

Analysis of the R wave transition

- If at V₁ → Left
- If V₂ or V₃ → Septal
- If at V₄ → Right

The fine algorithm then for exact localization of the accessory pathway

First step: Analysis of R wave transition

- V₁ → Left
- V₂ or V₃ → Septal
- V₄ → Right

Second step:

If left: Analysis of delta wave in leads I/avL

- Both leads -ve → LA
- Both leads positive → LP
- Only -ve in lead avL → LL

If septal: Analysis of delta wave in leads II, III & avF

- All leads +ve → RAS
- All leads -ve → Posteroseptal (then according to the R/S ratio V1 we differentiate between LPS and RPS)
- ve in leads III, avF and +ve in lead II → RMS

If right: Analysis of the delta wave III & avF

- ve → RP
- +ve → RA

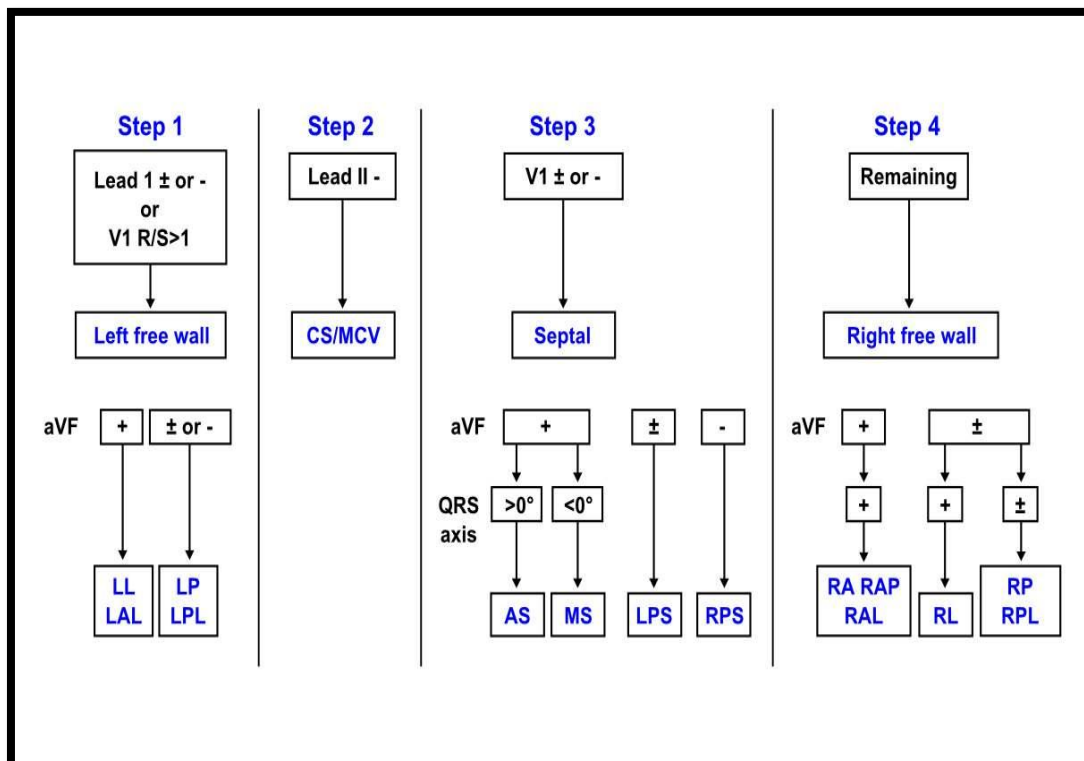


Fig. 1. Arruda algorithm. After Arruda M., Mccllelland J., Wang X., et al. [9]

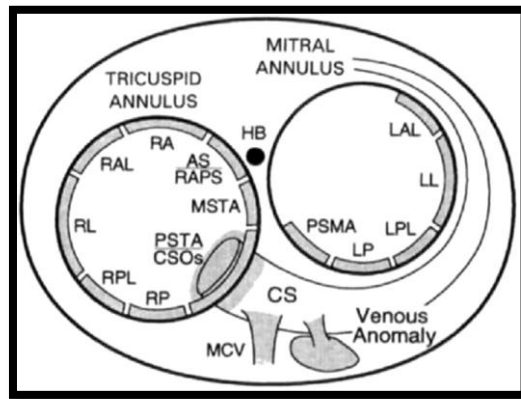


Fig. 2. A cross-section of the atrioventricular ring was shown in schematic drawings on the 30° LAO according to Arruda. After Arruda M., McClelland J., Wang X., et al. [9]

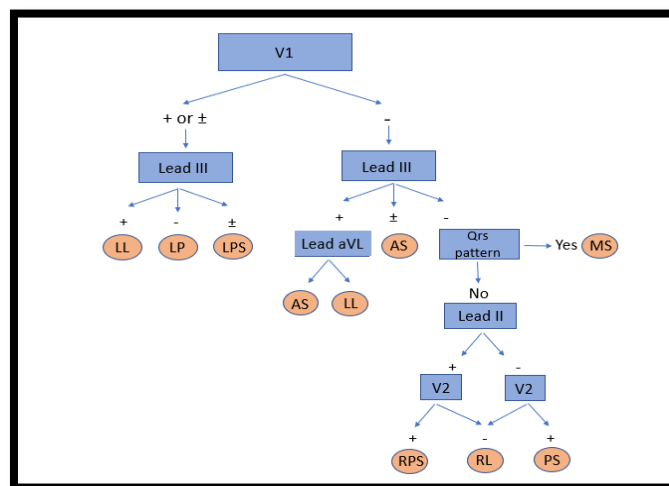


Fig. 3. d'Avila algorithm. After d'Avila A., Brugada J., Skeberis V., et al. [10]

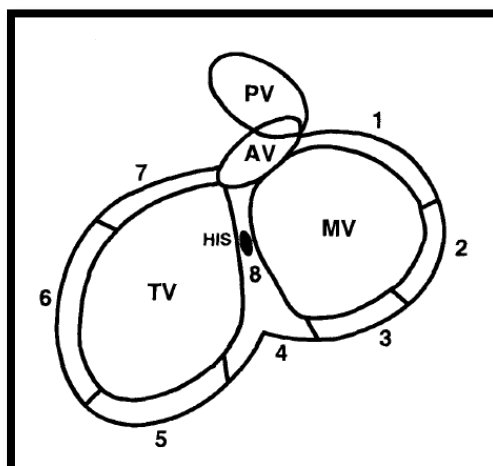


Fig. 4. Schematic drawings showing a cross-section of the atrioventricular ring on the 30° left anterior oblique projection. 1: left lateral AP; 2: left posterior AP; 3: left paraseptal AP; 4: posteroseptal AP; 5: right paraseptal AP; 6: right lateral AP; 7: anteroseptal AP; 8: midseptal AP; AV: aortic valve; MV: mitral valve; PV: pulmonic valve; TV: tricuspid valve [10]. After d'Avila A., Brugada J., Skeberis V., et al. [10]

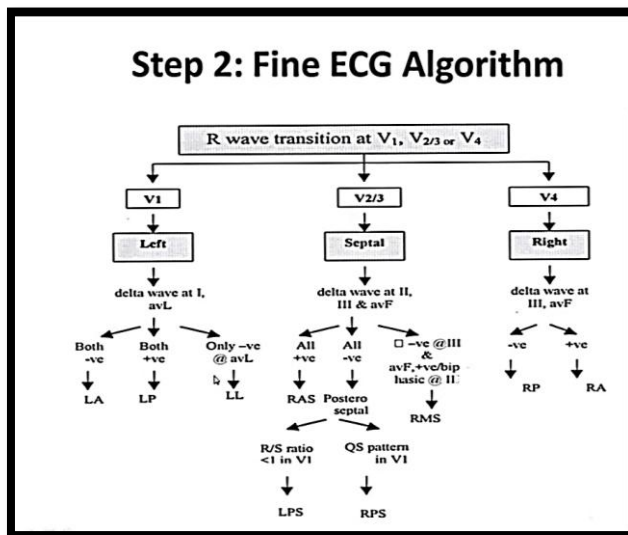
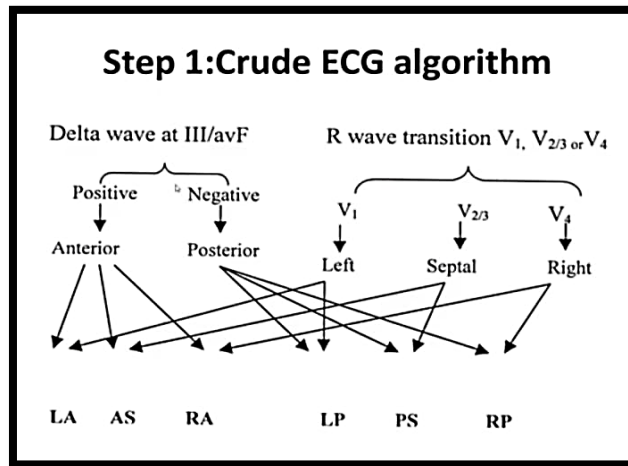


Fig. 5. Proposed algorithm

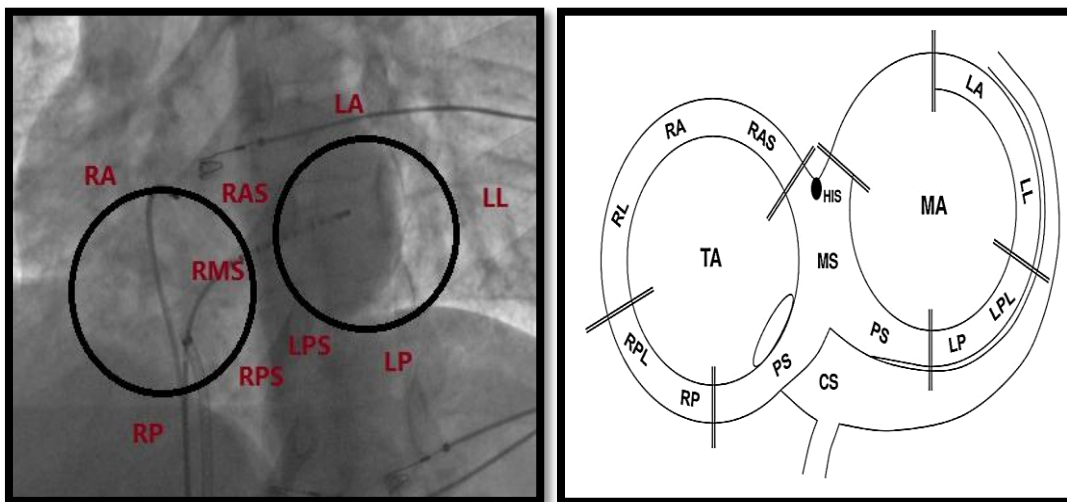


Fig. 6. Schematic drawings showed a cross-section of the atrioventricular ring on the 30° LAO according to the proposed algorithm

The ECG analysis process was done. The three algorithms were compared, and the fluoroscopy was used to locate the successful ablation location during catheter ablation. If more than one site was predicted by an algorithm, it might be a match if the precise location was among the options. It was permitted to count incorrect locations as nearby sites if they were close by the actual location. According to precise matches and nearby places, all of the algorithms were evaluated.

❖ Echocardiography

An echocardiogram was done using vivid- E9 echocardiography (GE) medical system equipped with M5S probe (frequency 1.7-3.3) MHz. at Tanta University Hospitals and using vivid- E9 at Demerdash hospital. Apical (4,3, and 2 chamber views) and parasternal views were acquired to detect any underlying cardiac disease. Left ventricular dimensions and ejection fraction were measured ($EF=SV/EDV$) [11].

❖ Electrophysiological study and radiofrequency catheter ablation:

A complete electrophysiological study was done on (Siemens) at Tanta University Hospitals and on (Siemens and Philips) at El Demerdash Hospitals. The study aimed for exact localization of the accessory pathway using four standard catheters, in the coronary sinus (CS), high right atrium (HRA), right ventricular apex (RVA), and HIS bundle site. The catheters were placed and adjusted in two standard angiographic views, right anterior oblique (RAO) and left anterior oblique (LAO) views.

2.4 Technique

▪ Patient preparation

The patient should first be informed about the steps and technique of the procedure and any concerns or questions should be addressed before the study, then an informed consent should be obtained.

▪ Steps

- 1- Sterilization & local infiltration of anesthesia using 10-20 cm lidocaine 1% close to the puncture site in the right groin.
- 2- First a femoral sheath (6-8 French (Fr)) is advanced through the femoral vein by manually locating the femoral artery in the region of the femoral triangle under the

inguinal ligament, followed by insertion of the needle just medial to the artery [12]. A total of three femoral vein sheaths (6-8 Fr) were placed, through which the catheters were advanced. Subclavian access was used in some patients.

3- Catheter placement: [13]

- ✓ **The coronary sinus catheter** which is a decapolar 6 Fr deflectable catheter was advanced through the femoral vein. RAO and LAO fluoroscopic views were used to guide catheter placement in the CS. Sometimes in case of non-deflectable catheters or in some right anterior APs, we needed to cannulate the CS from the SVC approach.
- ✓ **The His catheter** which is a quadripolar 6 Fr catheter was advanced utilising the RAO view, through the femoral vein into the RA, throughout the tricuspid annulus, until it becomes clearly in the RV. It was then pulled back throughout the tricuspid orifice while preserving a tiny clockwise torque to ensure proper connection with the septum until a His potential was received.
- ✓ **The RV catheter** which is another quadripolar 6F catheter was placed. The RV apex was most chosen for stability and reproducibility purposes.
- ✓ **The HRA catheter** (if needed) which is another quadripolar 6F catheter was used; with the tip of the RA catheter is positioned at the high posterolateral wall just at SVC-RA connection in the area of the sinus node or in the RA appendage. Sometimes a halo catheter was used.

4- Transseptal puncture: [14]

The femoral vein was used to get venous access, and then heparinized saline was used to flush out the guidewires, dilator, and sheath (8 Fr). With fluoroscopy supervision, the transseptal sheath-dilator assembly was pushed through into SVC to the height of the tracheal carina over just a J guidewire. After which the guidewire was removed, keeping the sheath as well as its dilator in place. In order to prevent the entrance of air into the RA, the dilator inside the

sheath was flushed and connected to a syringe.

The Brockenbrough needle was then inserted into the dilator while being continuously flushed until the needle tip was only 1 to 2 cm away from the tip of the dilator. In order to insert the tip of the dilator into the fossa ovalis, the sheath, dilator, and needle assembly were then twisted leftward and posteriorly with the needle's arrow pointing at 3 to 6 o'clock in relation to its shaft.

The dilator tip was therefore adjusted slightly leftward upon entering the RA and once again while descending into the aortic root with fluoroscopic supervision with a 30-degree LAO view. The crossing across the limbus and into the fossa ovalis is indicated by a third rapid leftward movement (the jump) underneath the aortic root. The needle was immediately moved to emerge outside the dilator in the LAO view once the location of the dilator tip at the fossa ovalis was established. The sheath-dilator-needle assembly was then gently pressed against the interatrial septum. We validate an intra atrial positioning of the needle tip inside the LA by injecting contrast via the needle to determine the location of the needle tip after passing through the fossa ovale and before advancing the dilator and sheath. A successful transeptal access is confirmed by opacification of the LA instead of the pericardium or aorta.

5- The electrophysiological study

A. Study during sinus rhythm:

- During sinus rhythm, ventricular pre-excitation is distinguished by a brief His bundle-ventricular (HV) or H-delta interval. His potential might be hidden in the ventricular electrogram of the area or Even negative HV intervals are possible. Early ventricular activation occurs close to the ventricular insertion point of the AP, or more specifically, close to the tricuspid or mitral annuli at the heart's base.
- Ventricular pacing (incremental pacing and VES): Retrograde ventricular pacing from RVA catheter to know pattern of atrial activation, induction of tachycardia and localize site of shortest V-A time.
- Atrial pacing (incremental pacing and AES): Antegrade atrial pacing from HRA or CS catheter to localize site of shortest A-V interval and induction of tachycardia.

- Other maneuvers (for example differential RV pacing and para-Hisian pacing) were used if needed to confirm diagnosis and to help exclusion of multiple accessory pathways.

- ✓ RV basal pacing vs RV apical pacing and monitoring the VA interval were used to perform differential RV pacing (i.e., the stimulus-to-atrial [SA] interval). A sequence of atrial activation to differential-site RV pacing is also seen. This procedure may prove or disprove the existence of a septal AV BT that is retrogradely conducting.
- ✓ The existence of a septal AV BT, which may facilitate an orthodromic AVRT with a retrograde atrial activation sequence similar to that during AVNRT, can be shown or disproved by para-Hisian pacing. By evaluating the SA interval between HB-RB capture and non-capture while preserving local ventricular capture and no atrial capture, the response to para-Hisian pacing may be studied.

B. Study during tachycardia (to confirm that the induced tachycardia during study is related to accessory pathway and to exclude presence of other tachycardias):

- Tachycardia cycle length.
- Pattern of atrial activation during the tachycardia (concentric or eccentric).
- VA time measurement (either more or less than 70 ms).
- Effects of BBB during orthodromic AVRT: A free-wall BT at the same side of the BBB is used to diagnose AVRT if the TCL and, more crucially, the surface VA interval are prolonged by >35 msec after the emergence of the BBB.
- Pacing from the RV apex during tachycardia at (20-40) ms was used to entrain from the RV apex for a number of beats before being discontinued.
- if the atrium was sped up to a similar pacing cycle length without altering the pattern of atrial activation and tachycardia persisted at the same cycle length after pacing was stopped. Post-pacing interval (PPI) measurement from the stimulus of the final RV pacing to the V electrogram of the next return beat. The A-H interval was assessed in the tachycardia just before to pacing.

- From the last atrial depolarization that was entrained to His electrogram in the first return beat, the post-pacing A-H interval was calculated. Because past entrainment affects the post-pacing A-H interval and changes the PPI, the increase in AV nodal conductivity in the first PPI (post-pacing A-H interval minus basal A-H interval) was removed from the PPI-TCL difference (corrected PPI-TCL difference). This PPI-TCL was labelled as being either more or less than 110ms after correction.

C. Electrophysiological Maneuvers for Localization of the Bypass Tract:

- Pacing From Multiple Atrial Sites:

A decrease in the P-delta interval throughout atrial pacing indicates proximity to the BT atrial insertion.

- Effects of BBB During Orthodromic AVRT:

A free-wall BT at the same side of the BBB is used to diagnose AVRT if the TCL and, more crucially, the surface VA interval are prolonged by >35 msec after the emergence of the BBB.

In relation to the establishment of BBB, supero-paraseptal and postero-septal BTs are connected to a reduced proportion of VA interval prolongation (about 5–25 ms) (for supero-paraseptal BT, RBBB; for postero-septal BT, LBBB).

- Mapping Ventricular Activation During Preexcited Rhythm:

The location of the BT ventricular insertion is determined by the location of the initial local ventricular activation (before to the commencement of the delta wave) along the mitral and tricuspid annuli.

- Mapping Atrial Activation During Retrograde Bypass Tract Conduction:

When performing orthodromic AVRT or ventricular pacing with backward

conduction across the BT, the location of the initial local atrial stimulation along the mitral and tricuspid annuli serves as a marker for the BT atrial insertion site.

- Mapping Bypass Tract Potential:

When performing orthodromic AVRT or ventricular pacing, the BT location can be determined by recording a BT potential 10–30 ms prior to the onset of the delta wave (during anterograde pre-excitation) or in the interval between the electrograms of the atria and ventricles at the first site of retrograde atrial activation.

6. Ablation was done at suspected site of accessory pathway using ablation catheter. Successful ablation will be confirmed by disappearance of manifest preexcitation in surface ECG. Also, full study was repeated after ablation to confirm successful ablation and exclude other tachycardia or multiple accessory pathways.

The location predicted by the three algorithms was compared to the exact location by electrophysiological study (which is the site of successful ablation in LAO 40-degree projection "gold standard") for assessment of sensitivity and specificity of each algorithm.

2.5 Statistical Analysis

With the aid of the IBM SPSS software package version 20.0, data were fed into the computer and evaluated. Number and percentage were used to describe qualitative data. The range (minimum to maximum), mean, standard deviation, and median were used to represent quantitative data. The 5% threshold of significance was used to determine the findings' significance.

3. RESULTS

The age of our patients ranged from 5 to 53 years, with mean value 25.95 years. There were 72 males (72%) and 28 females (28%). The study showed that 3 % of the studied cases were diabetic, 8% were hypertensive and 13 % of studied cases were smokers. The study showed that 83 % of the studied cases were symptomatic while the other 17 % were asymptomatic. The symptoms were palpitation, dizziness and syncope. Documented tachycardia was observed

in 63% of the cases in the form of pre-excited AF or supraventricular tachycardia (SVT). There was no documented tachycardia in remaining 37% of the studied cases. According to the Arruda algorithm, anteroseptal location of the accessory pathway was predicted in 38 cases, coronary sinus in 2 cases, left anterior/left anterolateral in 30 cases, left posterior/left posterolateral in 8 cases, mid septal in 2 cases, right anterior/right anterolateral in 4 cases, right lateral in 2 cases and right posteroseptal in 14 cases (Table 1).

Table 1. Distribution of accessory pathway locations predicted by Arruda algorithm

	Frequency (n)	Percentage (%)
AS	38	38.0
CS	2	2.0
LA / LAL	30	30.0
LP / LPL	8	8.0
MS	2	2.0
RA / RAL	4	4.0
RL	2	2.0
RPS	14	14.0
LPS	0	0.0
RP / RPL	0	0.0
Total	100	100.0

AS= anteroseptal, CS= coronary sinus, LA/LAL =left anterior/left anterolateral, LP/LPL = left posterior / left posterolateral, MS= mid septal, RA/RAL = right anterior /right anterolateral, RL = right lateral, RPS = right posteroseptal, LPS=left posteroseptal, RP/RPL = right posterior / right posterolateral

Table 2. Distribution of accessory pathway locations predicted by d'Avila algorithm

	Frequency (n)	Percentage (%)
AS	25	25.0
LL	33	33.0
LP	2	2.0
LPS	6	6.0
PS	11	11.0
RL	16	16.0
RPAS	7	7.0
MS	0	0.0
Total	100	100.0

AS= anteroseptal, LL=left lateral, LP = left posterior, LPS=left paraseptal, PS=posteroseptal, RL = right lateral, RPAS = right paraseptal, MS= mid septal

According to the d'Avila algorithm, the locations of the accessory pathways were classified as anteroseptal in 25 cases, left lateral in 33 cases, left posterior in 2 cases, left posteroseptal in 6 cases, posteroseptal in 11 cases, right lateral in

16 cases and right paraseptal in 7 cases (Table 2).

According to our proposed algorithm, 12 cases fulfilled the criteria as left anterior, 16 as left lateral, 4 as left posterior, 12 as right anterior, 34 as right anteroseptal, 4 as right mid septal, 2 as right posterior and 16 as right posteroseptal (Table 3).

Table 3. Distribution of accessory pathway locations predicted by our proposed algorithm

	Frequency (n)	Percentage (%)
LA	12	12.0
LL	16	16.0
LP	4	4.0
RA	12	12.0
RAS	34	34.0
RMS	4	4.0
RP	2	2.0
RPS	16	16.0
LPS	0	0.0
Total	100	100.0

LA= left anterior, LL=left lateral, LP = left posterior, RA =right anterior, RAS=right anteroseptal, RMS=right mid septal, RP = right posterior, RPS = right posteroseptal, LPS=left posteroseptal

Table 4. Distribution of exact accessory pathway locations by EP study

	Frequency (n)	Percentage (%)
CS	2	2.0
LA	6	6.0
LL	21	21.0
LP	14	14.0
RA	10	10.0
RAS	23	23.0
RP	4	4.0
RPS	20	20.0
LPS	0	0.0
RMS	0	0.0
Total	100	100.0

CS = coronary sinus, LA= left anterior, LL=left lateral, LP = left posterior, RA =right anterior, RAS=right anteroseptal, RP = right posterior, RPS = right posteroseptal, LPS=left posteroseptal. RMS=right mid septal

According to the exact electrophysiological site of ablation determined under fluoroscopy at 40-degree LAO projection, 2 cases were ablated inside the coronary sinus position, 6 at left anterior position, 21 at left lateral position, 14 at

left posterior position, 10 at right anterior position, 23 at right anteroseptal position, 4 at right posterior position and 20 at right posteroseptal position (Table 4).

According to the electrophysiological site of ablation determined under fluoroscopy and after dividing the accessory pathways into left (including LA, LAL,LP,LPL,LL), right (including RA, RAL,RL,RP,RPL and RPS) and septal (including RMS and RAS), 41 cases were ablated at left sided locations, 34 cases were ablated at right sided locations, 23 cases were ablated at septal locations and 2 cases only were ablated inside the coronary sinus (Table 5).

Table 5. Distribution of accessory pathway locations by EP study according to left, right, septal and CS APs

	Frequency (n)	Percentage (%)
Left sided AP	41	41.0
Right sided AP	34	34.0
Inside CS	2	2.0
Septal AP	23	23.0
Total	100	100.0

Table 6 represents the sensitivity, specificity, positive predictive value, and negative predictive value for each accessory pathway location according to the Arruda algorithm. For mid septal and left posteroseptal positions, sensitivity and positive predictive values could not be assessed as there no cases in our study were ablated at these sites. For the right posterior / right posterolateral locations, the sensitivity and positive predictive value was zero as Arruda algorithm couldn't predict these locations.

Table 6. Accuracy of the Arruda algorithm

Ablation site	Accuracy			
	Sensitivity (%)	Specificity (%)	+ve predictive value (%)	-ve Predictive value (%)
LP/LPL	57.1	100	100	93.5
LA/LAL	88.9	91.8	80	95.7
CS	0	98	0	98
AS	100	80.5	60.5	100
MS	-	98	-	100
LPS	-	100	-	100
RPS	70	100	100	93
RA / RAL	40	100	100	93.8
RL	100	100	100	100
RP / RPL	0	100	0	98

LP/LPL = left posterior / left posterolateral, LA/LAL =left anterior/left anterolateral CS= coronary sinus, AS = anteroseptal, MS= mid septal, LPS=left posteroseptal, RPS = right posteroseptal, RA/RAL = right anterior /right anterolateral, RL = right lateral, RP/RPL = right posterior / right posterolateral

Table 7 showed the accuracy of the D'Avila algorithm according to our study. The left posterior position sensitivity and positive predictive value were zero as d'Avila algorithm couldn't predict these locations in our cases. For mid septal position, sensitivity and positive predictive values could not be assessed as there no cases in our study were ablated at this site.

The accuracy of our proposed algorithm is shown in Table 8. For right mid septal and left posteroseptal positions, sensitivity and positive predictive values could not be assessed as there no cases in our study were ablated at these sites.

The sensitivity and specificity of each of the three algorithms is shown in Table 9 for left, right and septal position. For left sided accessory pathways, Arruda algorithm showed the highest specificity of 88.4% and our proposed algorithm showed the highest specificity of 100%. For right sided accessory pathways, d'Avila algorithm showed highest sensitivity values of 87.5%, but Arruda algorithm shows highest specificity of 100%. For septal accessory pathways: Our proposed algorithm and the Arruda algorithm showed the highest sensitivity of 100%, but the d'Avila algorithm showed the best specificity of 92%.

After adding the adjacent sites to the accurate sites, the total accuracy of the algorithms increased from 75% to 83% for Arruda algorithm, from 73% to 90% for d'Avila algorithm, and from 75 to 82% for our proposed algorithm.

Table 7. Accuracy of the d'Avila algorithm

AP location	Accuracy			
	Sensitivity (%)	Specificity (%)	+ve predictive value (%)	-ve predictive value (%)
LP	0	97.7	0	87.8
LL	86.2	88.7	75.8	94
AS	76	92	76	92
LPS	100	97.7	66.7	100
RPAS	50	97.8	71.4	94.6
RL	83.3	93.2	62.5	97.6
PS	100	98.9	90.9	100
MS	-	100	-	100

LP = left posterior, LL=left lateral, AS= anteroseptal, LPS=left paraseptal, RPAS=right paraseptal, RL = right lateral, PS=posteroseptal.MS= mid septal

Table 8. Accuracy of our proposed algorithm

AP location	Accuracy			
	Sensitivity (%)	Specificity (%)	+ve predictive value (%)	-ve Predictive value (%)
LP	28.6	100	100	89.6
LL	76.2	100	100	94
LA	100	93.6	50	100
RAS	100	85.7	67.6	100
RMS	-	96	-	100
LPS	-	100	-	100
RPS	80	100	100	95.2
RA	80.0	95.6	66.7	97.7
RP	50	100	100	98

LP = left posterior, LL= left lateral, LA = left anterior, RAS = right anteroseptal, RMS = right mid septal, LPS= left posteroseptal, RPS = right posteroseptal, RA=Right anterior, RP=right posterior

Table 9. Comparison between the three algorithms as regard left, right and septal positions

	Arruda		d'Avila		Proposed	
	Sensitivity %	Specificity %	Sensitivity %	Specificity %	Sensitivity %	Specificity %
Left sided AP	88.4	96.5	86.0	93.0	74.0	100
Right sided AP	58.8	100	87.5	91.2	82.4	97.0
Septal AP	100	77.9	76.0	92.0	100	80.5

4. DISCUSSION

The mean age of the patients was 25.95 ± 13.046 years. Most of the participants in the study were males (72%), this is also similar to Porter et al. [15] Studies showed that men are more likely to be affected by AVRT than women [16-17].

Regarding symptomatology, 83% of our patients were symptomatic while 17% were asymptomatic. Our study resembles Teixeira et al. [2], where 77.2% of his studied subjects were

symptomatic, and palpitation being the most frequently reported symptom.

Patients with AVRT like other supraventricular arrhythmias are mostly symptomatic, the most commonly reported symptoms are palpitations, or presyncope, dizziness, and chest pain [18].

Regarding the documented tachycardia, it was observed that 63% of our cases presented with pre-excited AF or supraventricular tachycardia (SVT). There was no documented tachycardia in remaining 37% of the studied cases.

Orthodromic AVRT presenting as narrow complex supraventricular tachycardias accounts for >90% of AVRTs, while antidromic AVRT also presenting as SVTs, but wide complex occurs in 3 - 8% of patients with WPW syndrome [19].

The presentation of WPW patients can also be in the form of preexcited AF, paroxysmal AF has been found in 50% of patients with WPW [20].

Regarding the exact electrophysiological site of ablation determined by fluoroscopy LAO 40 degree projection, our study showed that the majority of the cases were right anteroseptal representing 23 cases (23%) followed by 21 cases (21%) at left lateral position, 20 cases (20%) at right posteroseptal position, 14 cases (14%) at left posterior position, 10 cases (10%) at right anterior position, 6 cases (6%) at left anterior position, 4 cases (4%) at right posterior position and 2 cases (2%) were ablated at the coronary sinus position.

The majority of APs were found in the posteroseptal right region (28 participants, [25.20%]) and left lateral area (27 participants, [24.30%]), according to Teixeira et al.'s, [2] investigation. The sample has the least representation of the right anterolateral region (only one individual).

Teixeira et al. [2] and our study are parallel with the fact that despite the variety of AP subtypes, those that link the atria and the ventricles across the mitral or tricuspid annuli are the most popular. Around 15% insert along the right free wall, 25% along the septal side of the tricuspid or mitral annuli, and 60% are found along the mitral valve and are known as left free wall APs [18].

Regarding the total accuracy, our study showed that 73% of predictions were correct for d'Avila, 75% for Arruda, and 75% for our proposed algorithm. These findings are concordant with the results of Maden et al. [21] who found that 72.4 % for d'Avila, and 71.5% for Arruda.

Our study is again concordant with the study by Mostafa et al. [22] which showed that 81% of predictions were accurate for d'Avila, and 71% for Arruda.

Our proposed algorithm was similar to Arruda and D'Avila regarding the overall predictive accuracy. All three algorithms in this investigation predicted APs with a level of accuracy that was comparable. But according to the AP site, the

algorithms' accuracy was less accurate than what their inventors had claimed.

After adding the adjacent sites to the accurate sites, the total accuracy of the algorithms increased from 75% to 83% for Arruda algorithm, from 73% to 90% for d'Avila algorithm, and from 75 to 82% for our proposed algorithm.

This was again in line with the study by Teixeira et al. [2] which after adding the adjacent sites to the accurate sites showed the overall absolute accuracy of the algorithms evaluated significantly increased.

The improvement after adding the adjacent sites to the total accuracy was greatest for d'Avila algorithm, in our opinion this can be explained by the fact that the nomenclature of sites was the least (8 regions only compared to 13 for Arruda) which increased the chance of having more adjacent sites.

After dividing the accessory pathways into left (including LA, LAL, LP, LPL, LL), right (including RA, RAL, RL, RP, RPL and RPS) and septal (including RMS and RAS) accessory pathways, according to our study, Arruda algorithm showed that the highest sensitivity was for septal pathways and the highest specificity for right sided accessory pathways. d'Avila showed highest sensitivity and specificity for left sided accessory pathways, and our proposed algorithm showed highest sensitivity for septal pathways and highest specificity for left sided accessory pathways.

For left sided accessory pathways: Arruda algorithm showed the highest sensitivity of 88.4% and our proposed algorithm showed the highest specificity of 100%. For right sided accessory pathways: d'Avila algorithm shows highest sensitivity values of 87.5%, but Arruda algorithm shows highest specificity of 100%. For septal accessory pathways: Our proposed algorithm and the Arruda algorithm showed the highest sensitivity of 100%, but the D'Avila algorithm shows the best specificity of 92%.

According to Maden et al. [23] Arruda and Chiang were the two best algorithms for predicting right- and left-sided APs, respectively (p 0.001), if all predicted APs were categorized by the site (i.e., right-or left-sided, and midseptal/ anteroseptal). Arruda and d'Avila were the two most effective algorithms for accurately forecasting midseptal and anteroseptal APs (p 0.001).

In a pediatric population, Wren et al. [24] examined seven algorithms; they found that the d'Avila algorithm performed the lowest (with an accuracy rate of just 5%) in identifying midseptal and anteroseptal circuits.

Mostafa et al. [22] showed that for right APs, there was no significant difference between d'Avila and Arruda regarding the predictive accuracy.

5. CONCLUSIONS

Arruda & d'Avila's approach was the most effective at predicting left-sided accessory pathways, while d'Avila then our proposed algorithm were the best algorithms for prediction of accessory pathways at right-sided. The best algorithms for detection of anteroseptal and mid-septal accessory pathways were our proposed algorithm and Arruda.

To detect a WPW ventricular preexcitation, the ECG is a crucial diagnostic tool and important noninvasive tool for prediction of AP location. Prior knowledge of the AP location is essential to minimize unnecessary procedure manipulation and possible complications.

CONSENT

As per international standard or university standard, patient(s) written consent has been collected and preserved by the author(s).

ETHICAL APPROVAL

It is not applicable.

COMPETING INTERESTS

Authors have declared that no competing interests exist.

REFERENCES

1. Cai Q, Shuraih MS, Nagueh S. The use of echocardiography in Wolff–Parkinson–White syndrome. *The International Journal of Cardiovascular Imaging*. 2012;28(4): 725–734.
2. Teixeira C, Pereira T, Lebreiro CT, et al. Accuracy of the electrocardiogram in localizing the accessory pathway in patients with Wolff-Parkinson-White Pattern. *Arq. Bras. Cardiol*. 2016; 107(4): 331-338.
3. Icen Y, Donmez Y, Koca H, et al. Delta wave notching time is associated with accessory pathway localization in patients with Wolff-Parkinson-White syndrome. *J Interv Card Electrophysiol*. 2018;53:73-79.
4. Moss J, Gerstenfeld E, Deo R, et al. ECG Criteria for Accurate Localization of Left Anterolateral and Posterolateral Accessory Pathways. *PACE*. 2012;35:1444–1450.
5. Taguchi N, Yoshida N, Inden Y, et al. A simple algorithm for localizing accessory pathways in patients with Wolff-Parkinson-White syndrome using only the R/S ratio. *Journal of Arrhythmia*, 2014;30:439–443.
6. Williams B, Mancia G, Spiering W, et al. ESC/ESH Guidelines for the management of arterial hypertension The Task Force for the management of arterial hypertension of the European Society of Cardiology (ESC) and the European Society of Hypertension (ESH). *European Heart Journal*. 2018;39: 3021–3104.
7. American Diabetes Association. Classification and diagnosis of diabetes: Standards of Medical Care in Diabetes-2019. *Diabetes Care*. 2019;42:S13S28
8. Cheshire W. Syncope. *Continuum: Lifelong Learning in Neurology*. 2017; 23(2):335–358.
9. Arruda M, McClelland J, Wang X, et al. Development and validation of an ECG algorithm for identifying accessory pathway ablation site in Wolff- Parkinson-White syndrome. *J Cardiovasc Electrophysiol*. 1998;9(1):2-12.
10. d'Avila A, Brugada J, Skeberis V, et al. A fast and reliable algorithm to localize accessory pathways based on the polarity of the QRS complex on the surface ECG during sinus rhythm *PACE*. 1995 Sep;18(9 Pt 1):1615-27.
11. Arroyo JB, Schweickert AJ. Chapter 3 - Fluid Movement in the Body: Primer to the Cardiovascular System. 2013;43-66.
12. Iwashima S, Ishikawa T. & Ohzeki T. Ultrasound guided versus landmark-guided femoral vein access in pediatric cardiac catheterization. *Pediatr Cardiol*. 2008;29: 339–342.
13. Tanaka-Esposito C, Chung M, Abraham J, et al. Real-time ultrasound guidance reduces total and major vascular complications in patients undergoing pulmonary vein antral isolation on

- therapeutic warfarin. *J Interv Card Electrophysiol.* 2013;37:163–168.
14. Hsu J, Badhwar N, Gerstenfeld E, et al. Randomized trial of conventional transseptal needle versus radiofrequency energy needle puncture for left atrial access (the TRAVERSE-LA Study). *J Am Heart Assoc.* 2013;2:e000428.
 15. Porter M, Morton J, Denman R, et al. Influence of age and gender on the mechanism of supraventricular tachycardia. *Heart Rhythm.* 2004;1: 393_396.
 16. Lu C, Wu M, Chen H, et al. Epidemiological profile of Wolff_Parkinson_White syndrome in a general population younger than 50 years of age in an era of radiofrequency catheter ablation. *Int J Cardiol.* 2014;174:530-534.
 17. Rosano G, Leonardo F, De Luca F, et al. Cyclical variation in paroxysmal supraventricular tachycardia in women. *Lancet.* 1996;347:786_788.
 18. Brugada J, Katritsis D, Arbelo E, et al. ESC Guidelines for the management of patients with supraventricular tachycardia The Task Force for the management of patients with supraventricular tachycardia of the European Society of Cardiology (ESC). *European Heart Journal.* 2020; 41(5):655–720.
 19. Brembilla-Perrot B, Pauriah M, Sellal J, et al. Incidence and prognostic significance of spontaneous and inducible antidromic tachycardia. *Europace.* 2013;15:871-876.
 20. Etheridge S, Escudero C, Blaufox A, et al. Life-threatening event risk in children with Wolff-Parkinson-White syndrome: a multicenter international study. *JACC Clin Electrophysiol.* 2018; 4:433_444.
 21. Maden O, Balci K, Selcuk M, et al. Comparison of the accuracy of three algorithms in predicting accessory pathways among adult Wolff-Parkinson-White syndrome patients. *Journal of Interventional Cardiac Electrophysiology.* 2015;44(3):213–219.
 22. Mustafa M, Abo El Magd M. & Farh A. Comparison of the Accuracy of Three Algorithms in Predicting Accessory Pathways among Adult Wolff-Parkinson-White (WPW) Syndrome Patients in our Population. *The Egyptian Journal of Hospital Medicine.* 2018;72:5062-5066.
 23. Maden O, Balci K, Selcuk M, et al. Comparison of the accuracy of three algorithms in predicting accessory pathways among adult Wolff-Parkinson-White syndrome patients. *Journal of Interventional Cardiac Electrophysiology.* 2015;44(3), 213–219.
 24. Wren C, Vogel M, Lord S, et al. Accuracy of algorithms to predict accessory pathway location in children with Wolff- Parkinson-White syndrome. *Heart.* 2011;98(3): 202-6.

© 2022 Roshdy et al.; This is an Open Access article distributed under the terms of the Creative Commons Attribution License (<http://creativecommons.org/licenses/by/4.0>), which permits unrestricted use, distribution, and reproduction in any medium, provided the original work is properly cited.

Peer-review history:

The peer review history for this paper can be accessed here:
<https://www.sdiarticle5.com/review-history/94909>